Analysis of the π phase-shifts obtained in the Fourier spectra of phase gratings and grids by using two-window grating interferometry

N.-I. Toto-Arellano[a], G. Rodríguez-Zurita[b], A. Martínez García[a], J.F. Vázquez-Castillo[b], and J.A. Rayas Álvarez[a]

[a]*Centro de Investigaciones en Óptica, A.C.,*
Loma del Bosque #115 Col. Lomas del Campestre, Apartado Postal 1-948, 37150 León, Gto. México,
e-mail: ivantotoarellano@cio.mx
[b]*Facultad de Ciencias Físico-Matemáticas de la Benemérita Universidad Autónoma de Puebla,*
Apartado postal 1152, 72001 Puebla, Pue., México.

As it is very well known, the Fourier coefficients of only-phase gratings are Bessel functions of the first kind of integer order. Because the values of these real-valued functions oscillate around zero, they can adopt negative values, thereby producing phase shifts of π between some diffraction orders. To better understand the practical implications of this effect, in this work the phase shifts in the Fourier spectra of several phase gratings and grids are numerically found in order to compare them with experimental phase shifts. These experimental shifts induce changes in the modulation of the interference fringes formed by grating (or grid) interferometers when placing two windows at object plane of the system. Measurements of the changes in the interferograms are presented.

Keywords: Diffraction; phase grating; phase shift; interferometry; fringe analysis; Bessel function.

Es conocido, que los coeficientes de Fourier de rejillas de fase son funciones de Bessel de la primera clase de orden entero. Ya que los valores de estas funciones reales oscilan alrededor de cero, entonces pueden adoptar valores negativos, de tal manera que pueden producir cambios de fase de π entre algunos órdenes de difracción. Para entender mejor las implicaciones prácticas de este efecto, en este trabajo se encuentran numéricamente los corrimientos de fase en el espectro de Fourier de varias rejillas y mallas de fase y son comparadas con los corrimientos de fase experimentales. Estos corrimientos de fase inducen cambios en la modulación de franjas de los patrones de interferencia formados por interferómetros de rejilla (o malla) al colocar dos ventanas en el plano del objeto del sistema. Se presentan mediciones de los cambios surgidos en los interferogramas.

Descriptores: Difracción; rejillas de fase; corrimiento de fase; interferometría; análisis de franjas; funciones de Bessel.

PACS: 42.87.Bg; 42.79.Ci; 42.79.Dj; 42.15.Eq; 42.25.Hz; 07.05.Pj

1. Introduction

Phase gratings have been employed as an optical element with more diffraction efficiency than absorption gratings to perform a variety of tasks. Among them we find splitting for interferometry, intensity measuring [1] and optical shop testing [2,3]. The performance of phase gratings depends strongly upon their Fourier spectra. The case of sinusoidal phase grating has been discussed for a long time [4], so it is well known that its Fourier coefficients are Bessel functions of the first kind of integer order q, J_q [5]. Such functions are real valued and their values oscillate around zero; hence they can introduce π phase-shifts in a given grating Fourier spectrum. These shifts are of little relevance, if any, to applications where the power spectrum results as the main concern, as is often the case in spectroscopy [6]. But recently it has been pointed out that a grating interferometer with two windows at the object plane performs as a common path interferometer [7]. Several advantages have been shown, such as its mechanical stability [8,9]. Two-window phase-grating interferometers (TWPG) are based on the interference between neighboring diffraction orders [7]. Thus, the fringe contrast of each interference pattern can be affected when π phase-shifts are presented [10]. Furthermore, these phase shifts have to be taken into account for the overall performance of the system and can influence its design even with practical advantages [10]. This note is aimed at the phase changes between diffraction orders that have been observed in the Fourier spectra of a phase grating. To show the variety of Fourier spectra that it is possible to attain, some examples of sinusoidal phase gratings are calculated with a standard FFT routine. This would serve for the interpretation of the experimental observations reported. Because some experimental consequences of phase shifts appear also in phase grids, the corresponding discussion for sinusoidal phase gratings follows. Experimental observations in agreement with the previous discussions are then shown by using commercial phase gratings.

2. Basic considerations

A TWPG is depicted in Fig. 1. Basically, it consists of a $4f$ Fourier optical system, being f the focal length of each transforming lens. Illumination comes from a YVO_4 laser operating at 532 nm. Two windows (**A** and **B**) are placed at the object plane (x, y), while a periodic phase-only transmittance $G(u/\lambda f, v/\lambda f)$ is placed at the frequency plane (u, v). Then, μ and ζ are the frequency coordinates scaled

to the wavelength λ and the focal length. At the plane (u, v), the period of G is denoted by d, and its spatial frequency by $\sigma = 1/d$. Two neighboring diffraction orders thus have a distance of $X_0 = \lambda f/d$ at the image plane. Then, $\sigma \cdot u = X_0 \cdot \mu$.

2.1. Sinusoidal phase gratings

The complex amplitude of a plane, sinusoidal phase grating placed at the Fourier plane of a $4f$ system can be expressed as

$$G_1(\mu, \zeta) = e^{i2\pi \cdot A_g \sin[2\pi X_0 \mu]}$$

$$= \sum_{q=-\infty}^{\infty} J_q(2\pi A_g) e^{2\pi q X_0 \mu}, \qquad (1)$$

with $2\pi A_g$ being the grating phase amplitude and J_q the Bessel function of the first kind of integer order q. The Fourier transform of Eq. (1) is then given by

$$\tilde{G}_1(x, y) = \sum_{q=-\infty}^{\infty} J_q(2\pi A_g)\delta(x - qX_0, y), \qquad (2)$$

with $\delta(x, y)$ being the two-dimensional Dirac delta function. Thus, the Fourier spectrum of a sinusoidal phase grating comprises point-like diffraction orders of amplitude weighted by Bessel functions. Such spectrum can be detected at the image plane of the $4f$ system.

2.2. Phase grids

A sinusoidal phase grid can be generated by the multiplication of two sinusoidal phase gratings whose respective grating vectors are forming an angle of 90 degrees. Taking the rulings of one grating along the "μ" direction, and the rulings of the second grating along the "ζ" direction, the resulting phase grid can be written as

$$G_2(\mu, \zeta) = e^{i2\pi \cdot A_g \sin[2\pi X_x \mu]} e^{i2\pi \cdot A_g \sin[2\pi X_y \zeta]} \qquad (3)$$

$$= \sum_{q=-\infty}^{\infty} J_q(2\pi A_g) e^{2\pi q X_0 \mu} \sum_{r=-\infty}^{\infty} J_r(2\pi A_g) e^{2\pi r X_0 \zeta},$$

where the frequencies along each axes directions are taken as $X_x = X_y = X_0$. By convolving the Fourier transform of both gratings, the Fourier transform of the phase grid becomes

$$\tilde{G}_2(x, y) = \sum_{q=-\infty}^{\infty} \sum_{r=-\infty}^{\infty} J_q(2\pi A_g) J_r(2\pi A_g)$$

$$\times \delta(x - qX_0, y - rX_0), \qquad (4)$$

which are point-like diffraction orders distributed on the image plane on the nodes of a lattice with a period given by the value X_0.
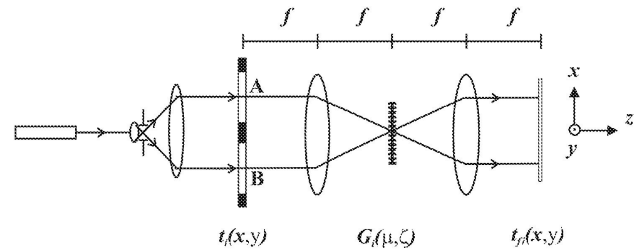

FIGURE 1. TWPG with phase periodic element G of period X_0.

3. Two-window phase-grating interferometry: interference-pattern contrasts and modulation

Phase grating interferometry is based on a phase grating placed as the pupil of a $4f$ Fourier optical system [7-11]. The use of two windows at the object plane in conjunction with phase grating interferometry allows interference between the optical fields associated to each window with higher diffraction efficiency [7,10,11]. Such a system performs as a common path interferometer (Fig. 1). A convenient window pair for a grating interferometer implies an amplitude transmittance given by

$$t_1(x, y) = w\left(x + \frac{x_0}{2}, y\right) + w'\left(x - \frac{x_0}{2}, y\right), \qquad (5)$$

where x_0 is the separation from center to center between two rectangular windows. One rectangular aperture, $w(x, y)$, can be written as $w(x, y) = rect[x/a] \cdot rect[y/b]$, and the second one as $w'(x, y) = w(x, y) \exp\{i\phi(x, y)\}$, while a relative object phase is described with the function $\phi(x, y)$. As shown in Fig. 2, a and b represent the side lengths of each window (**A** and **B**). Placing a grating of spatial period $d = \lambda f/X_0$ at the Fourier plane, the corresponding transmittance is given by $G_1(\mu, \zeta)$. The image formed by the system consists basically of replications of each window at distances X_0, that is, the convolution ($*$) of $t_1(x, y)$ with the point spread function of the system, defined by $\tilde{G}_1(x, y)$. This results into the following

$$t_{f1}(x, y) = t_1(x, y) * \tilde{G}_1(x, y)$$

$$= \sum_{q=-\infty}^{\infty} J_q(2\pi A_g) w\left(x + \frac{x_0}{2}, y\right) * \delta(x - qX_0, y)$$

$$+ \sum_{q=-\infty}^{\infty} J_q(2\pi A_g) w'\left(x - \frac{x_0}{2}, y\right) * \delta(x - qX_0, y).$$

By adding the terms q and $q - 1$ [both located within the same replicated window $w(x - X_0[q - 1/2], y)$], and for the case of matching the windows positions with the diffraction order positions ($X_0 = x_0$), the previous equation simplifies to

TABLE I. Bessel coefficients sign relations of superimposed orders. Case of $\phi(x, y) = 0$.

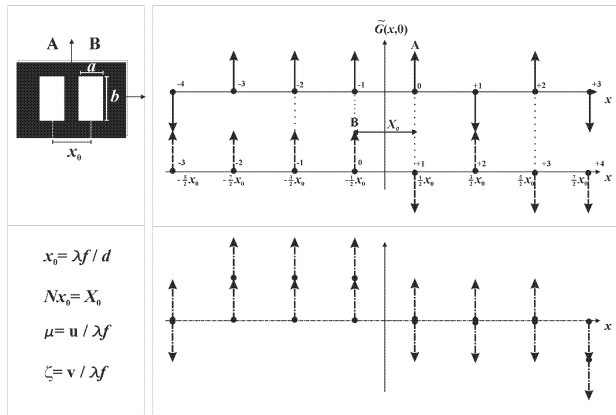| $q = 0$	$J_0 + J_{-1} = J_0 - J_1$	$q = -1$	$J_{-1} + J_{-2} = -J_1 + J_2$
$q = 1$	$J_1 + J_0$	$q = -2$	$J_{-2} + J_{-3} = J_2 - J_3$
$q = 2$	$J_2 + J_1$	$q = -3$	$J_{-3} + J_{-4} = -J_3 + J_4$
$q = 3$	$J_3 + J_2$	$q = -4$	$J_{-4} + J_{-5} = J_4 - J_5$

FIGURE 2. Amplitude of diffraction orders in the image plane of a TWPG resulting from a window displacement of $\pm x_0/2$. Window geometry (upper left).
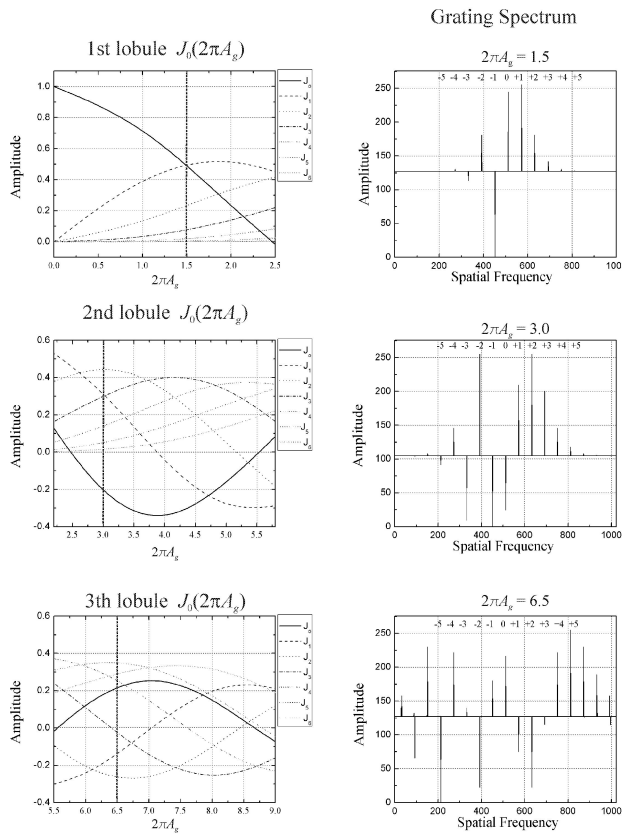

FIGURE 3. Fourier spectra of phase gratings: left column, Bessel region (first seven Bessel functions shown), right column, grating spectra.
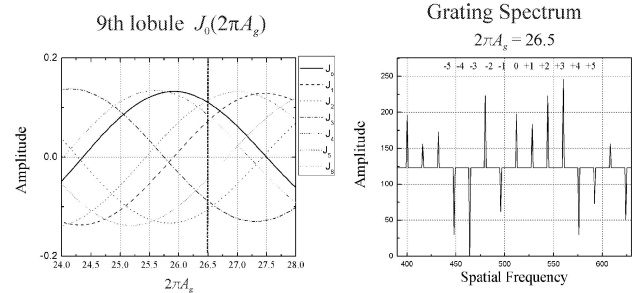

FIGURE 4. Fourier spectrum of a phase grating. Case: ninth lobule.

$$t_{f1}(x, y) = \sum_{q=-\infty}^{\infty} \left[J_q(2\pi A_g) w\left(x - x_0[q - 1/2], y\right)\right]$$

$$+ \sum_{q=-\infty}^{\infty} \left[J_{q-1}(2\pi A_g) e^{i\phi(x - x_0[q-1/2], y)}\right.$$

$$\left. \times w\left(x - x_0[q - 1/2], y\right)\right]. \tag{6}$$

Thus, an interference pattern between fields associated to each window must appear within each replicated window. The fringe modulation m_q of each pattern would be of the form

$$m_q = \frac{2 J_q J_{q-1}}{J_q^2 + J_{q-1}^2}. \tag{7}$$

3.1. π-shifts of the Fourier spectra of sinusoidal phase gratings

According to Eq. (7), the modulation of each interference pattern depends on the relative phases of J_q and J_{q-1}. Thus, the signs of J_q are also relevant. For the case of $\phi(x, y) = 0$, this relation is shown in Table I for some cases of q. For cases of $q = 0, -1, -2, -3, -4$, a negative contrast is expected; otherwise, it would be positive.

The interference pattern contrast is positive for one half of the diffraction orders if the grating's Fourier coefficients are all positive for $q > 0$, whereas the other half will show alternating contrasts due to the odd parity of J_{2q+1}. These results can also be depicted as in Fig. 2, where only the diffraction orders from a given grating are separately shown as displaced from the origin due to the respective displacement of windows **A** and **B** (first two plots from above the top). The case of $J_4 < 0$ is shown. For simplicity, the replicated windows are not plotted. The third row in the graph exhibits the superposition of the two previous spectra. Contrast changes appear

in both halves of the image plane. The expected signs of each fringe contrast in this case would be +,-,-,-,+,+,+,- from left to right.

3.2. Some examples of calculated Fourier spectra: sinusoidal phase gratings

In order to show some cases of phase-shifts in grating spectra, several fast Fourier transforms have been calculated for gratings of different phase amplitudes A_g. We use the lobules of J_0 as a reference to indicate the Bessel region within which the amplitude A_g of the corresponding phase grating is to be found. Only seven Bessel functions are shown in Fig. 3. In the first case, within the first lobule of J_0, the associated spectrum results with one half of its Fourier components in phase, while the other half show phase shifts of π in an alternating way. In this region, J_0 is positive and in phase with the Fourier components of the first half above mentioned. For the second case, J_0 is negative. Taking a value of A_g such that the Bessel functions with $q = 1...6$ adopt only positive values, the Fourier spectrum of the resulting grating turn out to be similar to the first case, J_0 being negative as the only different phase shift. Within the 3rd lobule, it is possible to pick up negative values for $q = 1, 2, 3$, the resulting Fourier spectrum showing π-shifts accordingly. In Fig. 4 we show a case of positive values for $q = 1, 2, 3$, and negative for $q = 4, 5$.

This situation corresponds to a region within the $9th$ lobule of J_0. The varieties of shifts suggested by the previous simulations are in agreement with Eq. (7). When using this type of gratings in a TWPG, the corresponding interference contrast around each diffraction order can be obtained with plots similar to the ones in Fig. 2.

3.3. π-shifts of the Fourier spectra of sinusoidal phase grids

A rectangular phase grid can be generated with two phase gratings of equal spatial frequency. Fig. 5a depicts the signs of the diffraction orders of a grid made up from two crossed gratings having spectra as the one in Fig. 2. Positive signs are denoted with hollow circles, whereas negative signs are marked with crosses. The dashed lines form regions enclosing diffraction orders of index pairs $0, n$ or $m, 0$. Then, order $0, 0$ is located at the intersection of these regions. Several possible configurations of windows can be considered for a TWPG. Two of these configurations are shown in Fig. 5b. They are denoted by W_1 and W_2. Respective displacements of diffraction patterns are also indicated with displaced dashed lines.

For the case of phase grids with windows in configuration W_2, the image can be written as:

$$t_{f2}(x,y) = t_2(x,y) * \tilde{G}_2(x,y) = \sum_{q=-\infty}^{\infty} \sum_{r=-\infty}^{\infty} w\left(x + \frac{x_0}{2}, y + \frac{x_0}{2}\right) * J_q(2\pi A_g)J_r(2\pi A_g)\delta(x - qX_0, y - rX_0)$$

$$+ \sum_{q=-\infty}^{\infty} \sum_{r=-\infty}^{\infty} w'\left(x - \frac{x_0}{2}, y - \frac{x_0}{2}\right) * J_q(2\pi A_g)J_r(2\pi A_g)\delta(x - qX_0, y - rX_0),$$

Again, with $X_0 = x_0$

$$t_{f2}(x,y) = \sum_{q=-\infty}^{\infty} \sum_{r=-\infty}^{\infty} J_q(2\pi A_g)J_r(2\pi A_g)w\left(x + \frac{x_0}{2}[1 - 2q], y + \frac{x_0}{2}[1 - 2r]\right) \tag{8}$$

$$\times \sum_{q'=-\infty}^{\infty} \sum_{r'=-\infty}^{\infty} J_{q'}(2\pi A_g)J_{r'}(2\pi A_g)w'\left(x + \frac{x_0}{2}[1 + 2q'], y + \frac{x_0}{2}[1 + 2r']\right).$$

where

$$t_2(x,y) = w\left(x + \frac{x_0}{2}, y + \frac{x_0}{2}\right) + w'\left(x - \frac{x_0}{2}, y - \frac{x_0}{2}\right).$$
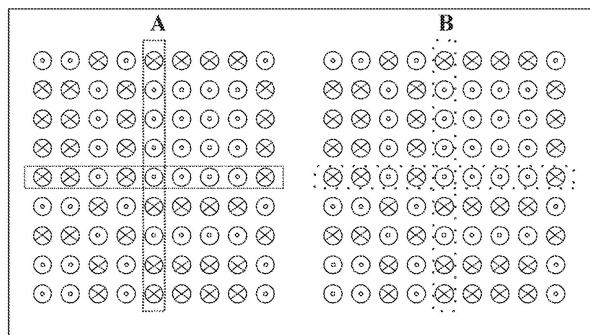
With $q' = q - 1, r' = r - 1$, this result simplifies to

$$t_{f2}(x,y) = \sum_{q=-\infty}^{\infty} \sum_{r=-\infty}^{\infty} \left[J_q(2\pi A_g)J_r(2\pi A_g) + J_{q-1}(2\pi A_g)J_{r-1}(2\pi A_g)e^{i\phi(x-x_0[q-1/2],y-x_0[r-1/2])}\right] \tag{9}$$

$$\times w\left(x - x_0[q - 1/2], y - x_0[r - 1/2]\right).$$

Similarly as for gratings, the fringe modulation of the interference pattern within a window centered in $(x_0[q - 1/2], x_0[r - 1/2])$ is
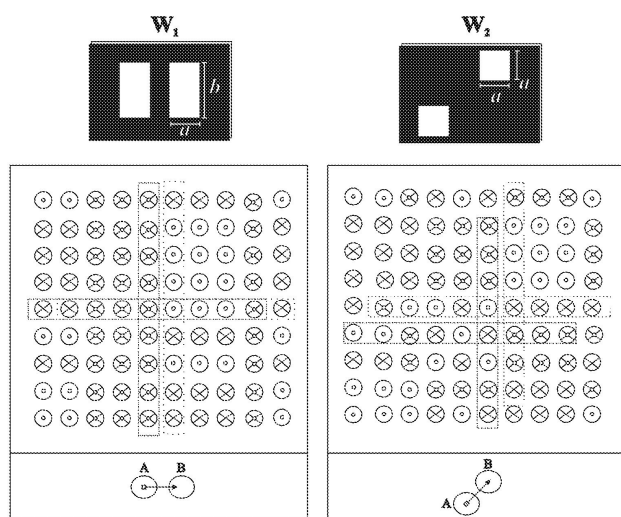
$$m_{qr} = \frac{2J_q J_{q-1} J_r J_{r-1}}{(J_q J_r)^2 + (J_{q-1} J_{r-1})^2}. \tag{10}$$

TABLE II. Phase shifts measured of experimental patterns of Fig.6 according to the method from Kreis.

steps	g_0	g_1	g_2	g_3	g_4	g_5	g_6	g_7
(Standar steps								
is π)	0	3.150	3.130	3.510	0.005	0.014	0.008	3.154

(a)

(b)

FIGURE 5. a) π-phase distribution of diffraction orders of grids. b) TWPG order superpositions: Configuration W_1 : interference pattern signs for displaced windows along the x-axis. Configuration W_1: interference patterns signs for displaced windows along a line at 45°.
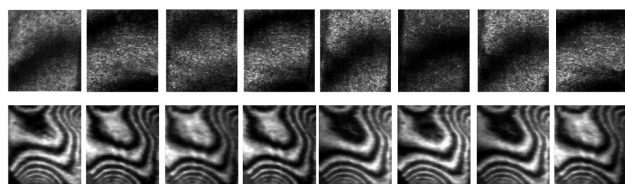

FIGURE 6. Two experimental sets of interferograms with a phase-grating.

TABLE III. Phase shifts measured of experimental patterns of Fig. 7 according to the method from Kreis (square in dashed lines).

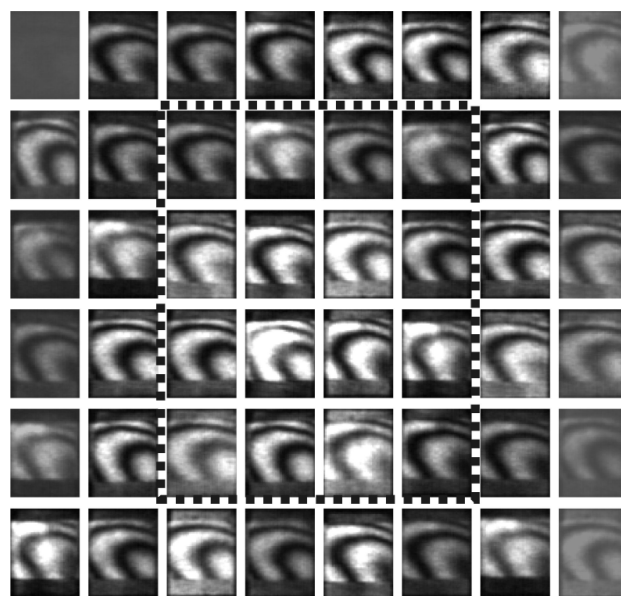|	Shifts (rad)		
0.026	0.015	3.174	3.133
0.038	0.002	3.153	3.164
3.136	3.135	0.000	0.024
3.131	3.158	0.020	0.031

FIGURE 7. Experimental patterns for a phase-grid (composite image, windows configuration W_2).

4. Experimental testing of the phase-shifts in phase gratings and phase grids

Figure 6 shows the superposition of Fourier amplitude spectra under windows configuration W_1 for a phase grating with 110 lines/mm. The contrast of the corresponding experimental interference patterns can be interpreted as if its first four Fourier coefficients had phase relations as the ones sketched in Fig. 4. They were obtained with the system in Fig. 1. Two different situations are depicted, one on the upper row (a small tilt in one window) and another on the lower row (oil on glass). The patterns show the relative phases of the diffraction orders discussed in previous sections (modulation with signs +,-,-,-,+,+,+,- from left to right). The phase-shifted steps of the experimental fringe patterns can be calculated by

applying the algorithm proposed by Kreis [12]. The resulting mean values for the upper row of interferograms are shown in Table II. It can be seen from the table that they depart by small amounts from π or 0.

For the case of the diffraction orders belonging to a phase-grid constructed with two crossed gratings of equal frequency, the corresponding interference patterns are shown in Fig. 7 for windows configuration W_2. Each grating gives patterns as in Fig. 6 when placed in the system of Fig. 1. The whole image is a composite image because patterns of higher order have low intensities. The contrasts are in agreement with the conclusions derived from Fig. 5. The relative phase values of the 16 patterns shown within the square drawn with dashed lines in the patterns of Fig. 7 employing the method from Kreis can be seen in Table III. Configuration W_1 gives pattern contrasts in agreement with Fig. 5b (they are not shown). The use of a grid as a beam divider having as a result several interferograms resembles some shearing interferometers proposed earlier [13], but ours is not a shearing system.

5. Final remarks

Theoretical and experimental evidence of π-shifts in the Fourier spectra of phase gratings and phase grids were pre-

sented. These shifts are not discussed in the literature as far as we know. The usual focus on the power spectrum tends to hide the effect, but it can be of considerable relevance when using gratings or grids for interferometric applications, for example: in phase shift interferometry, these results are convenient since only one grating displacement is necessary to capture four interferograms and for the case of polarization phase shifting interferometry, the characteristics of the phase gratings under study simplify the placement of polarization filters and allow us to obtain of n-patterns in one shot with adjustable phase shift.

1. R.M.A. Azzam, *Opt. Acta* **29** (1982) 685.

2. V. Ronchi, *Appl. Opt.* **3** (1964) 437.

3. A. Cornejo-Rodríguez, *Ronchi Test*, c.9 in Optical Shop Testing, 2nd edition (D. Malacara edition, Wiley, New York, 1992) p. 321.

4. E.S. Barrekette and H. Freitag, *IBM Journal* (1963) 345.

5. J.W. Goodman, *Introduction to Fourier Optics*, 2nd edition (McGraw-Hill, 1988).

6. F. Kneubühl, *Appl. Opt.* **8** (1969) 505.

7. V. Arrizón and D. Sánchez-De-La-Llave, *Opt. Lett.* **29** (2004) 141.

8. C. Meneses-Fabian, G. Rodriguez-Zurita, and V. Arrizon, *JOSA A* **23** (2006) 298.

9. C. Meneses-Fabian, G. Rodriguez-Zurita, and V. Arrizon, *Opt. Commun.* **264** (2006) 13.

10. G. Rodriguez-Zurita, C. Meneses-Fabian, N.I. Toto-Arellano, J. Vázquez.Castillo, and C. Robledo-Sánchez, *Opt. Express* **16** (2008) 7806.

11. P.W. Ramijan, "Processing Stereo Photographs by Optical Subtraction", *Ph. D. Thesis*, University of Rochester (1978).

12. T. Kreis, *J. Opt. Soc. Am. A* **3** (1986) 847.

13. M.V. Mantravadi, *Lateral shearing interferometers*, c.4 in Optical Shop Testing, 2nd edition (D. Malacara editor, John Wiley and Sons, New York 1992) p. 123.